Journal of Sustainable Energy & Environment
13 (2022) 47-57

Experimental investigation of external PV slats for daylighting in Thailand

Damson Daniel Kadete, Pipat Chaiwiwatworakul* and Surapong Chirarattananon

The Joint Graduate School of Energy and Environment, King Mongkut's University of Technology Thonburi, Bangkok, Thailand
Center of Excellence on Energy Technology and Environment (CEE), Ministry of Higher Education, Science, Research and Innovation, Bangkok, Thailand
*Corresponding author. Tel.: +66-816-592-535, Fax: +00-000-000
E-mail address: pipat.cha@kmutt.ac.th

Abstract: This paper presents an investigation of the daylighting from external multiple shading slats integrated with photovoltaics (PV). Experiments were carried out at an outdoor chamber with a south-facing window. Based on the measured results using various sensors, the daylighting characteristics were analyzed for an office environment under varying tropical sky conditions. Relationships of the exterior daylight illuminance and the interior daylight distribution could be empirically formulated, and they were used to determine the required artificial light from electric lamps to supplement the transmitted daylight from the window. In the assessment of the daylighting potential of the PV shading slats, a monthly adjustment scheme of the slat angle to fully intercept the direct sunlight from the south window was proposed together with the task-ambient lighting concept. By using our experimental room as the demonstration case, the analysis showed that the daylighting of the PV slat system could reduce the lighting energy consumption by 80% compared to the typical office case designed with the uniform lighting concept. The generated solar energy from the PV array on the slat surface was estimated to be sufficient for the lighting by the direct-current LED lamps. However, battery storage was required due to the time mismatch between the solar power generation and the required electricity for supplement lighting.

Keywords: Daylighting, dimmable lighting, PV slats, tropical climate, workplane illuminance.

1. Introduction

Climate change and global warming are the critical environmental challenge that requires collaborations from all countries to mitigate the greenhouse gas (GHG) emission from fossil fuel burning and from various business activities. According to the International Energy Agency (IEA) report, building sector consumed 35% of the global final energy and it shared up to 38% of the total emitted GHG [1]. Energy efficiency and renewable energy use are perceived as the two complementary strategies that curb the increasing sectoral energy demand and lead a city to meet the carbon neutrality target.

Geographically, Thailand is present in the tropical climate zone around the earth equator where the natural daylight is abundant, and the solar irradiance is intensive. The highly luminous sky together with the long daylength over a year are advantageous to the natural daylight use for interior illumination in buildings [2-3]. The observations from a meteorological station in Bangkok reported that the hourly mean value of the global daylight illuminance exceeded 10 klux from 8:00 a.m. and reach 80klux noontime [4].

Appropriate daylighting technologies such as electrochromic glaze, light pipe, laser cut panel, etc. have been developed for the tropics [5]. However, as the sun travels in all orientations in the region, multiple shading slats are a simple but effective device for controlling the daylight transmission and the solar gain into buildings. Different installations have been investigated for example the slats affixed behind the window, the slats located in front of the window, or a specific configuration of the slats placed between the two glazing panes. In operation, the slats might be permanently fixed at a position or capably tilted to a different angle.

A study in Jordan used a simulation software, namely Lightscape, to determine the daylight illuminance on the work plane level (0.75 m above floor) in an office of which the window was south-facing and equipped with fixed external horizontal slats [6]. The results showed that the daylight distribution in the room with the shaded window had better space visual quality, as opposed to the case of non-shaded window, since the slats could modify the daylight distribution depending on the tilted angle.

In the tropics, the daylighting of the automated Venetian blind located between the two glazed panes was assessed by conducting physical experiments in an outdoor chamber under varying condition of the real sky [7-8]. The observed results were used to validate the developed daylighting model. The evaluation showed that the slats could conserve electrical energy up to 70% compared to the uniform lighting with a full reliance on electric lamps. Noted that the remarkable saving was achieved by the advancement of automatically slat adjusting with respect to the outdoor daylight to maintain the required indoor illuminance of 500 lux.

It is found that the external shading slats were a focus of some studies particularly in the tropics, as the slats could intercept the beam solar irradiance before incident on the windowpane; giving a better thermal performance, as compared to the internal installation. Ingabo et al. evaluated the adjustable external horizontal slats for daylighting from the south window in Thailand by conducting the full-scale experiments and the software simulations [9]. The study results established the appropriate monthly slat angle adjustment and determined that installation of adjustable external shading slats could save up to 60% of total lighting and air-conditioning energy consumption compared to workspaces with unshaded heat reflective glass windows. The same authors also had a separate research work for the north window [10]. The energy saving of 50% could be achieved, slightly lower than the south-facing window case.

Building integrated photovoltaic or BIPV is a renewable energy technology that reduces the building energy consumption

by the electricity generated from the solar energy resource. Considered as a class of the BIPV, the photovoltaic shading device (PVSD) in a particular form of the multiple PV slats could function for both the daylighting and power generation. In Italy, characteristics of different fixed external PV shading devices were analyzed, and suggestion of geometric parameters were provided [11] while optimization for multi-purpose objective of fixed shading slats on minimizing electricity use, maximizing PV generation, and maximizing daylighting were provided in simulation study by considering number of blades and tilt angle [12]. However, in other research it was noted that external fixed shading device provide low level of daylight in overcast days and sometimes causes penetration of direct solar radiation therefore occupants prefer adjustable shading slats [13].

Other than the technology advancement itself, the means of interior illumination in office space could significantly influence the energy saving potential. In a typical building, the interior lighting is full reliance on the electric lamp based on the uniform work plane light level for the whole space. The daylight provision is also designed to meet the lighting requirement of the uniform lighting concept. In order to achieve a low-energy building, task-ambient light offers a sufficient light provision to comply to the lighting standard with a lower energy consumption. The concept is to provide sufficient light level of about 300lux for general or circulation area and the higher illuminance at 500lux for only the working stations. The daylighting from the window will be designed to serve the circulation area. The additional lighting from electric lamp will serve the working stations.

In this paper, the daylight application of the shading slats integrated with photovoltaics (PV) was investigated for the south-facing window. Physical experiments were carried out to observe the system characteristics and the interior daylight distribution. A set of empirical models were then developed and then used to assess the potential of energy saving from the daylighting for an office space. A simple slat adjustment scheme together with task-ambient lighting concept was demonstrated for achieving a low energy building.

2. Methodology

2.1 The PV shading slats

A prototype of the PV slats was fabricated and equipped with a south-oriented window of an experimental chamber. The slats, each of which had a dimension of 3.0m length by 0.3 m width, could be altered to any tilted angle from 0° of the fully open to 90° of the completely close using a linear actuator driven by a programmable logic controller (PLC). The shading slats were painted white. Figure 1(a) illustrates a photo of the PV slat installation.

A total of one hundred fifty-four monocrystalline PV cells were affixed on the slats, and all were wired in series for electricity generation. Physically, the installed PV cells occupied approximately 50% of the slat upper surface. According to the specification, the rated voltage and current of each PV cell was 0.37 V and 0.05 A at the standard testing condition, respectively.

2.2 Experiments

Full-scale experiments were carried out at an outdoor chamber of 9.0 m length by 3.0 m width. The floor-to-ceiling height was 2.65m. As shown in Fig. 1, three sets of the double-pane low-emissivity glazing window were situated on the south-facing wall, having the aggregate dimension of 2.7 m width by 1.95m height. The windowsill was 0.7 m above the floor. The window-to-wall ratio was calculated at 0.74 (south wall). Other walls of the chamber were fully opaque. The interior surfaces of the room ceiling and walls were painted white with a visible reflectance of 0.7. The floor reflectance was measured at 0.4. A fan coil unit was installed to condition the room at the setpoint temperature of 25°C.

Four experiments were set each for a distinct slat angle of 0°, 30°, 50° and 70°. Figure 1(b) shows the light sensor positions inside the chamber to observe the interior daylight from the shaded windows. The transmitted daylight was measured by a light sensor placed vertically behind the glazed window. Other sensors were used to measure the daylight illuminance on the work plane level for five points along the room center at 10%, 30%, 50%, 70% and 90% room depth. The incident solar irradiance on the PV cell was simultaneously measured by a pyranometer.

(a) The PV shading slats

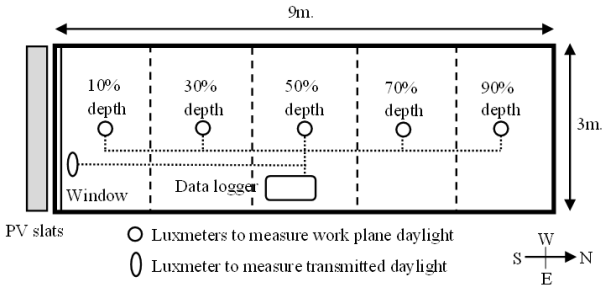

(b) Sensor installation

Figure 1. The PV slats system for the experimental daylighting study.

The amounts of the exterior daylight illuminance and the solar irradiance were measured at a meteorological station nearby the experimental site (latitude 13.7°N and longitude 100.44°E). The provided data included the global, diffuse horizontal and beam normal daylight illuminance and solar irradiance together with the vertical daylight and irradiance on the four cardinal orientations: north, east, south, and west. The temperature and relative humidity of the ambient air were also measured. The data was recorded at one-minute intervals and the recording time was synchronized with that of the experimental data acquisition system. No tall structure offered any obstruction to the station.

2.3 Assessments

Daylighting performance of the PV slats was assessed in aspects of the available daylight at the study location, the workplane daylight illuminance, the supplement lighting electricity, and the power generation from the PV slats. The energy saving from the daylighting was appraised opposed to the traditional practice of the uniform lighting for office.

a) Daylight availability

Amount of exterior daylight is climate dependent. Its availability is the necessary primary data source for daylighting design, technology development, and performance assessment. In Thailand, a ground-based station has performed the routine measurements of the global, diffuse horizontal, and beam normal daylight illuminance in Bangkok. The total daylight illuminance on vertical planes oriented to north, east, south, and west were simultaneously measured, and recorded at one-minute interval. All the records were also subject to a procedure of the data quality

assurance. This study employed the records from the station to determine the local daylight availability on the windowed façade and used it to assess the daylighting of the PV shading slats.

b) Transmitted daylight

Mechanism of the daylight transmission through the external multiple slats is complicated due to various influences that are the directional behavior of the beam daylight illuminance, the anisotropic distribution of the sky luminance, the geometrical position of the slats relative to the sun, and the visual properties of the slat surface. In Fathoni, 2016 [8], an accurate calculation of the transmitted daylight was presented by which the analysis of the beam component was separated from the diffuse component. The thirteen CIE standard sky models were adopted to account for non-uniform luminance distribution of the real sky. And, by assuming the diffusive slat surface, the flux transfer method could be applied to determine the daylight inter-reflection between the two adjacent slats.

In this study, the correlation between the exterior daylight on the windowed façade and the transmitted daylight through the PV slats was investigated based on the diagram given in Fig. 2. According to the diagram, the variable S_1 represented the mounted PV cells on the slats. S_2 and S_3 were the upper and the lower surfaces of the slats, respectively. These three sections (S_1, S_2 and S_3) had the visible reflectance corresponding with the PV cell and the slat surfaces. S_4 was a fictious surface of the luminous source of which the leaving light flux, called the exitance (M_4), was equal to the total vertical daylight illuminance (E_s); meaning that the surface had the transmittance of 100% (the surface reflectance was 0%). The section S_5 represented the glazing pane of the window with the visible reflectance of ρ_w and the visible transmittance of τ_w.

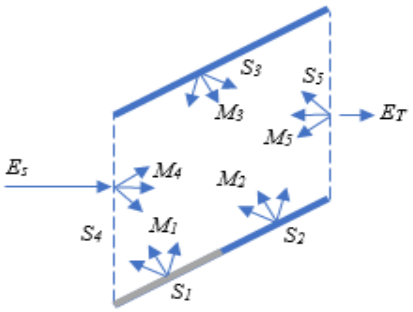

Figure 2. The daylight transmission through the PV shading slats.

As shown in Fig. 2, the daylight exitance M_4 of the surface S_4 travelled and reached other surfaces S_2 to S_5. Then, the incident daylight was further reflected to all other surfaces. This multiple reflection would perform until the daylight energy was completely absorbed by the surfaces. As all the surfaces were assumed to be diffusive, the phenomenon could be explained by the flux transfer method using Eq. (1):

$$M_i = M_{di} + \rho_i \sum_{j=1}^{n} F_{ij} M_j \tag{1}$$

where

M_i is final exitance inclusive of the direct exitance of surface i

M_{di} is initial exitance of surface i

ρ_i is reflectance of surface i

F_{ij} is form factor from surface i to j

As the value of ρ_1 for the fictious surface S_1 was 0, so the value of the final exitance M_1 was equal to the initial exitance M_{d1} and was also equal to the vertical daylight in the windowed façade E_s. For the surfaces S_2 to S_5, the initial exitance (M_{di}) could be derived by multiplying their surface reflectance with the corresponding direct illuminance (E_{di}) received from the luminous surface of S_1. Equation 2 exemplified the calculation of the initial exitance of the surface S_5 (M_{d5}) or the window surface:

$$\begin{aligned} M_{d5} &= \rho_5 \cdot E_{d5} \\ &= \rho_5 \cdot F_{45} \cdot M_4 \end{aligned} \tag{2}$$

By solving the multiple linear equations, the final exitance M_5 and the transmitted daylight from the shaded window were then determined by Eq. (3) and (4), respectively:

$$\begin{aligned} M_5 = &(\rho_5 \cdot F_{45} \cdot M_4) + (\rho_1 \cdot F_{15} \cdot M_1) \\ &+ (\rho_2 \cdot F_{25} \cdot M_2) + (\rho_3 \cdot F_{35} \cdot M_3) \\ &+ (\rho_4 \cdot F_{45} \cdot M_4) \end{aligned} \tag{3}$$

$$E_T = \tau_w \cdot \frac{M_5}{\rho_5} \tag{4}$$

According to Eqs. (1)-(4), the transmitted daylight (E_T) could be represented by a proportion with the vertical daylight on the windowed facade E_w with respected to the slat angle. Regarding the directional daylight characteristic and the anisotropic sky luminance distribution, their influences could be accounted by the resulting vertical daylight illuminance and the relatively low surface reflectance of the PV slats.

In the physical experiment study, the total daylight illuminance on the windowed façade (south orientation) and the transmitted daylight were measured by the light sensors to observe their correlation at different tilted angle of the PV slats.

c) Workplane daylight

The interior daylight on the work plane (0.75m above the floor) were investigated in terms of the illuminance value and the distribution pattern along the room depth from the windowed wall. With this regard, the work plane was divided into five sub-sections as shown in Fig. 1(b). For a situation, any points on the work plane directly received the daylight from the window considered as the lighting source. The points also received the reflected daylight from all other room surfaces due to the multiple light reflection as described in previous sub section for the PV slats. Similar calculation approach of the flux transfer method could be used at the first step to determine the final exitance of all interior surfaces (walls, floor, ceiling, window). The work plane daylight illuminance at different points is the summation of the luminous flux leaving from the window (source) and those leaving from the surfaces as expressed by Eq. 5:

$$E_{vd} = E_T \cdot C_i + \sum_{i=1}^{n} M_i \cdot C_i \tag{5}$$

where C_i is a configuration factor of the interior surface and the given point on the work plane. The first term of Eq. 5 represents the illuminance from the window while the second term represents the illuminance from the room surfaces. In this study, the experiments were carried out to measure the workplane daylight at 10%, 30%, 50%, 70%, and 90% depth of the room and then determined their correlation with the transmitted daylight.

d) Electric lighting

Energy efficient LED lamps are currently used in commercial office buildings. In this study, the LED lamps were assumed to be installed on the ceiling of the model room to provide uniform

illumination on the workplane. The lamp efficacy was reasonably approximated at 100 lm/W. Based on the IESNA lumen method illustrated by Eq. 6, the calculation indicated the lighting power density (LPD) was 10.58 W/m^2 for the required workplane illuminance 500lux as shown in Table 1.

$$E_w = (LLF)(CU)\left(\frac{L_f}{P}\right)\left(\frac{P}{A}\right) \quad (6)$$

where E_w is target workplane illuminance, *LLF* is light loss factor (assumed to be 0.8), *CU* is coefficient of utilization (assumed equal to 0.8), L_f/P is the lamp efficacy and *P/A* is lighting power density.

Table 1. Specific information of the light luminaire.

Total light flux (lm)	2680	
Total power (W)	26.8	
Efficacy (lm/W)	100	
Work plane luminance (lux)	300	500
Lighting power density (W/m^2)	6.35	10.58

Dimmable lamps are uncommon in typical office buildings. However, this daylighting study assumed that a dimming controller was integrated with the lighting system to regulate the light from lamps to supplement the daylight from the slat window. With this control, LPD of the lighting system varied linearly with light flux from lamps.

e) Power demand

Electricity is consumed when the electric lamps are switched on. The lamps themselves also dissipate heat that finally contribute to the additional cooling load of the air-conditioner. In this paper, the resulting power demand could be calculated by Eq. (7):

$$P = \left(LPD + \frac{LPD}{COP}\right) \cdot A_f \quad (7)$$

where *LPD* stands for the average lighting power density (W/m$_{fl}^2$), A_f are the areas of the floor area (m$_{fl}^2$). *COP* is the coefficient of performance of the air-conditioner assumed to be equal to 3.0.

The calculation postulated that the amount of the dissipated heat from the lamps was equal to their electrical energy supply. With this regard, the resulting power demand from lighting was increased by 30% to accounting for the indirect power from air-conditioning.

3. Results and Discussion

3.1 Experimental results

a) Case 1: 0° slat angle

Figure 3 exhibits a series of plots of the one-minute experimental results of the PV slats at 0° angle. The global daylight illuminance (E_{vg}) was recorded with a peak value of 85 klux around noon (Fig. 3(a)). The diffuse daylight illuminance (E_{vd}) from sky was low and not exceeding 20 klux, indicating that

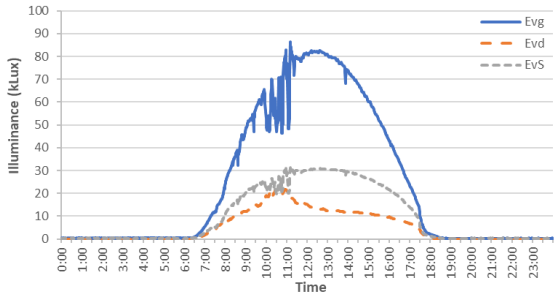

(a) Daylight illuminance

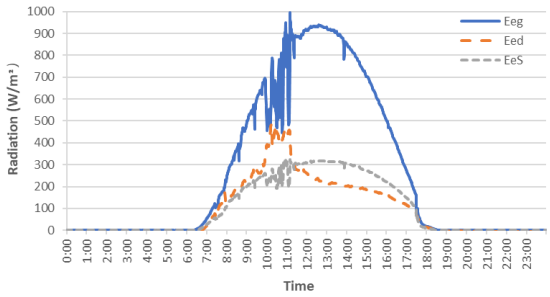

(b) Solar irradiance

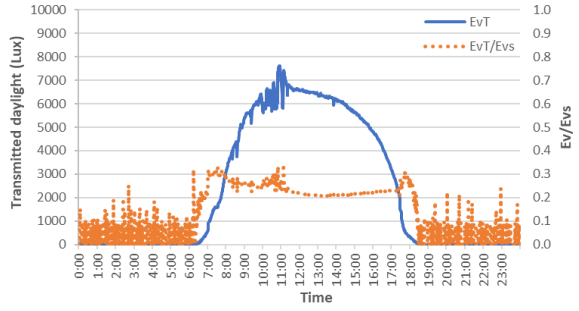

(c) Transmitted daylight from the window

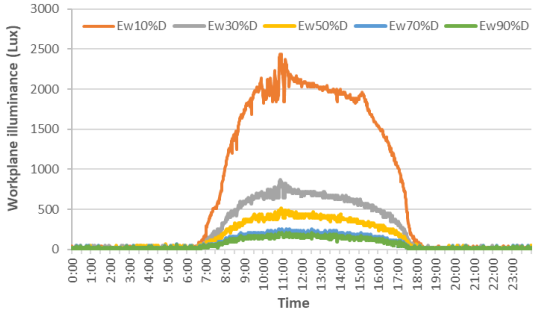

(d) Workplane daylight illuminance

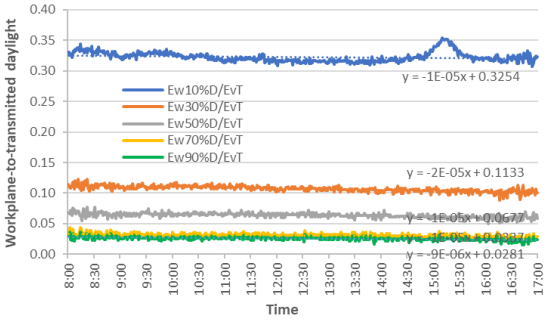

(e) The workplane to transmitted daylight ratio

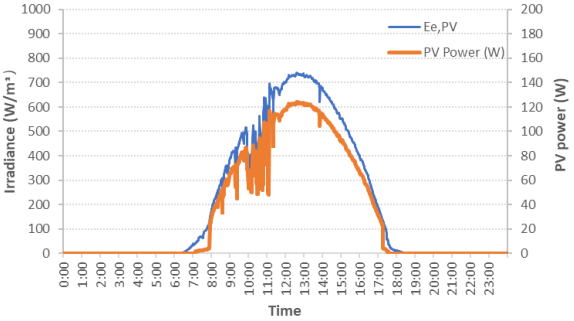

(f) Solar irradiance and power of the PV array

Figure 3. The slats at the angle of 0°.

the sky was rather clear over the day. However, the appearance of the large fluctuation in the plot informed of the presence of moving clouds during 9:30-11:30. The vertical daylight on the south-facing windowed façade (E_{vs}) varied correspondingly and had its peak at 30 klux. Figure 3(b) presents the measured solar irradiance of which the variation patterns (the global (E_{eg}), the diffuse horizontal (E_{ed}), and the south oriented (E_{es}) solar irradiance) were similar to their daylight illuminance counterparts.

Figure 3(c) shows the transmitted daylight from the window (E_{vT}). The maximum value was observed at around 7,000 lux. Superimposed in the figure, the ratio of the transmitted to the total daylight on the windowed façade (E_{vT}/E_{vs}) were found to vary within a narrow range of 0.2-0.3 throughout the office hours. This result pointed out that 70 up to 80% of the total vertical daylight was shaded by the PV slats.

The workplane daylight illuminance at 10%, 30%, 50%, 70%, and 90% of the room depth (D) were plotted in Fig. 3(d). Their values near the window (i.e., $E_{i10\%}$) exceeded the standard illumination level of 500 lux for the task lighting in office space. The values were actually as high as 2,000 lux for most office period. The workplane daylight at the middle zone of the room (i.e., $E_{i50\%}$) still exceeded 300 lux, and it was sufficient for the ambient lighting. However, as the workplane daylight exponentially dropped along the room depth, its values fell below 300 lux near the rear wall (i.e., $E_{i90\%}$).

According to Fig. 3(e), the interior daylight distribution was presented by using the ratio of the workplane daylight at different points in the room to the transmitted daylight from the window (E_i/E_{vT}). It was obvious that the workplane daylight could be simply determined by using the value of E_i/E_{vT} which was constant for any particular room point. In this experimental case, the values of E_i/E_{vT} at 10%D, 30%D, 50%D, 70%D, and 90%D were equal to 0.325, 0.113, 0.067, 0.030, and 0.028, respectively.

The incident solar irradiance on the PV cell ($E_{e,PV}$) of the upper slat surface measured by a pyranometer. In Fig. 3(f), the variation of the incident irradiance seemed identical to the global irradiance (E_{eg}) rather than the vertical south-facing irradiance (E_{es}). The solar power from the PV slats varied corresponding to the incident irradiance and had its peak at 150 W_{elec}. It was observed that the solar irradiance threshold of the power generation was about 100W/m^2. *b) 30° slat angle*

The observed exterior daylight and solar irradiance during the 30° angle experiment are given in Figs. 4(a) and 4(b). Their variation patterns were rather similar to that of the 0° angle experiment; however, more clouds were present in the morning (7:30-11:00). The amounts of the exterior daylight and solar irradiance were almost the same as the previous experiment.

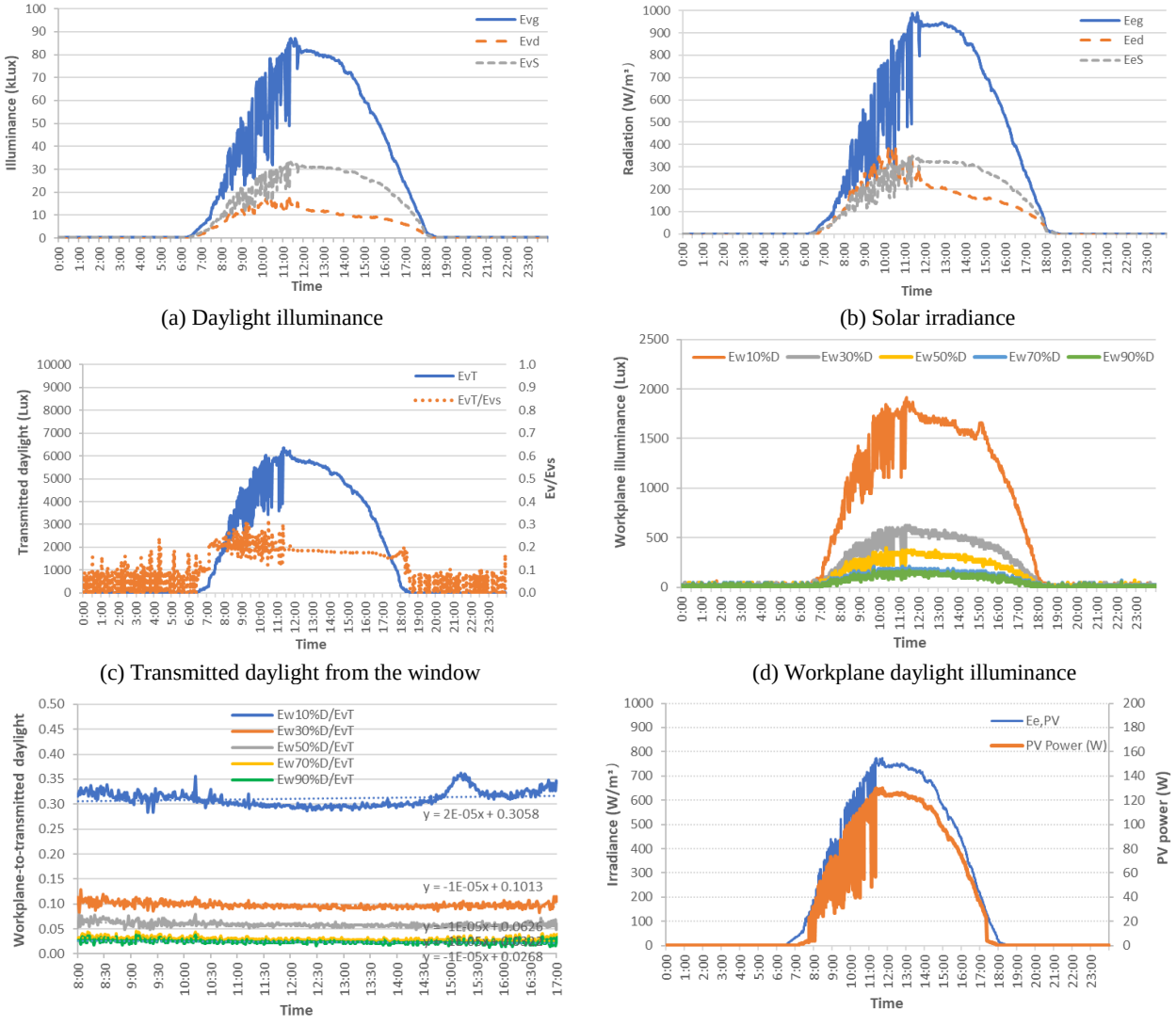

(a) Daylight illuminance

(b) Solar irradiance

(c) Transmitted daylight from the window

(d) Workplane daylight illuminance

(e) The workplane to transmitted daylight ratio

(f) Solar irradiance and power of the PV array

Figure 4. The slats at the angle of 30°.

The transmitted daylight was presented in Fig. 4(c). The value of E_{vT}/E_{vs} was about 0.19, obviously lower than that of the 0° angle experiment. This was because the PV slats were now altered to a higher tilted angle (30°) to intercept the vertical daylight on the windowed façade at a greater extent. Figure 4(d) shows the lower illuminance level of the workplane daylight as compared to that of the 0° angle experiment. The maximum daylight at the 10% depth was 1800 lux. However, the distribution describing in term of E_i/E_{vT} seemed to be identical for both experiments. By considering the solar irradiance on the PV array, the measurements showed a well comparison for both experiments.

c) 50° slat angle

The exterior daylight and solar irradiance in this experiment were distinct from the previous two experiments. The sky was partly cloudy in the morning as it was observed from the large varying daylight amount. Then, the sky was overcast throughout the afternoon. Under the presence of the partly cloudy sky condition, the exterior daylight was still quite high.

Figure 5(c) as compared to Fig. 3(c) and 4(c), the transmitted daylight further decreased with the increasing slat angle. The value of E_{vT}/E_{vs} was about 0.13 at the PV slat angle of 50. As it could be expected, the daylight illuminance values on the work plane were again lower. However, the proportion of E_{vi}/E_{vT} was found to be well maintained.

Here, it should be noted that the experimental results of the 70° angle were not presented in this paper, as they were rather similar to that of the 50° angle. For these two angles, the slats were almost fully close.

d) Daylighting of the PV slats

By the above experiments, the results demonstrated that the daylight on the south facing facade was abundant. The corresponding solar irradiance was also intense due to the incident beam component. The PV slats could perform to be an effective device of the interior daylight control whilst generating power to serve the supplement electric lighting.

To further analyze the PV slats application, Fig. 6(a) shows a relationship of E_{vT} and E_{vs} with respect to the slat angle (θ), derived from the experimental measurements. The relationship of E_i and E_{vT} was also observed as given in Fig. 6(b).

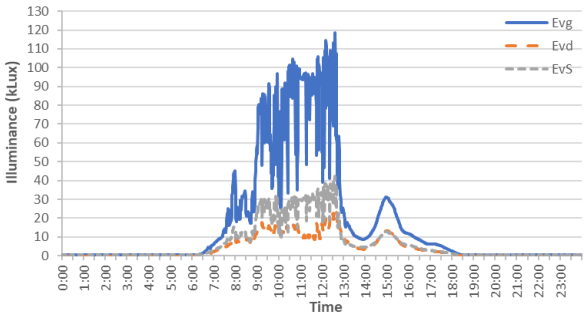

(a) Daylight illuminance

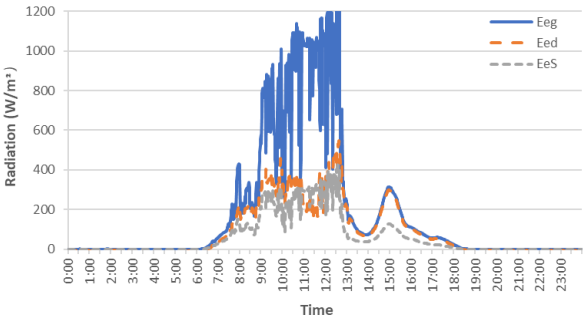

(b) Solar irradiance

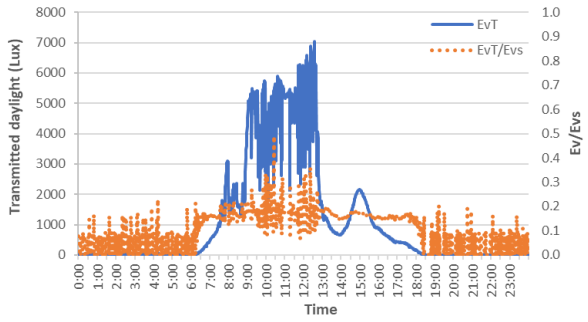

(c) Transmitted daylight from the window

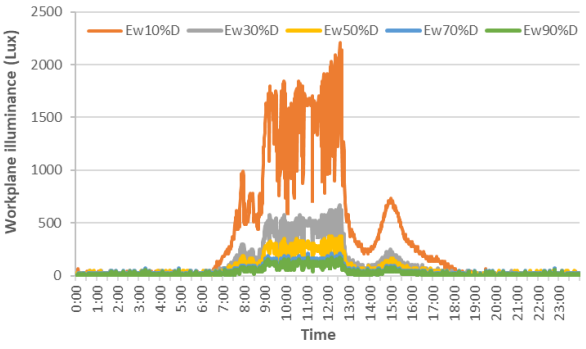

(d) Workplane daylight illuminance

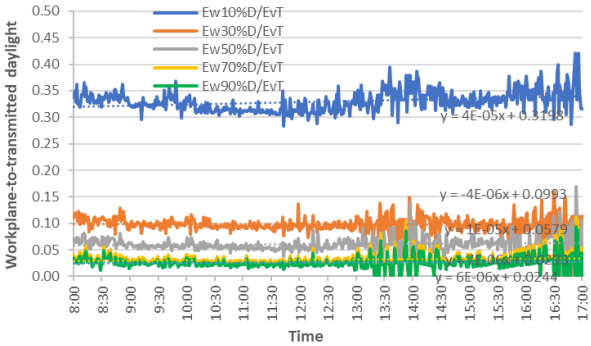

(e) The workplane to transmitted daylight ratio

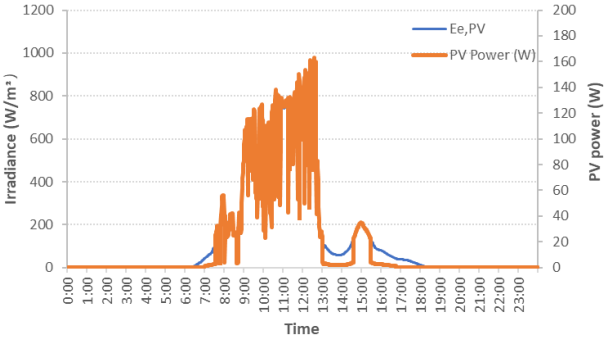

(f) Solar irradiance and power of the PV array

Figure 5. The slats at the angle of 50°.

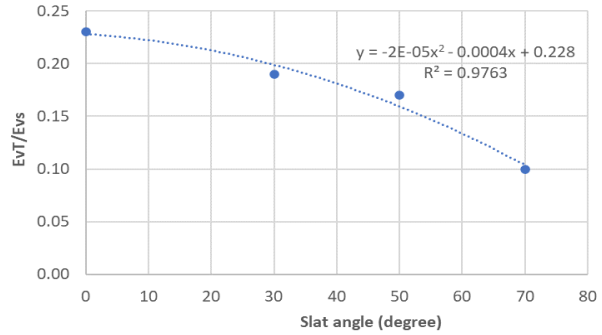

(a) E_{vT}/E_{vs} as a function of the slat angle

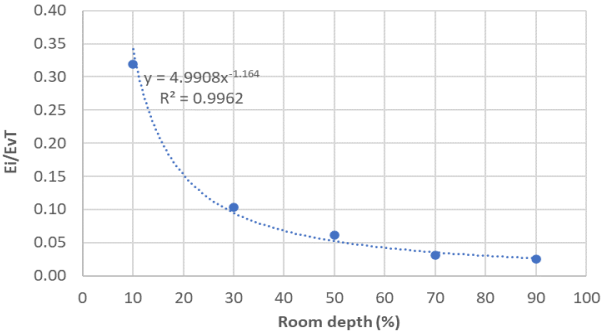

(b) E_i/E_{vT} as a function of the room depth

Figure 6. Daylighting characterization of the PV slats.

The two relationships could be expressed by Equations (8) and (9) below:

$$\frac{E_{vT}}{E_{vs}} = (-2\times10^{-5})\cdot\theta^2 - 0.0004\cdot\theta + 0.228 \quad (8)$$

$$\frac{E_{w,x}}{E_{vT}} = 4.9908\cdot\left(\frac{x}{D}\right)^{-1.164} \quad (9)$$

Figure 7 shows the relationship of the electrical power generated from the PV slats with respect to the global irradiance. As can be observed, the power generation was activated when the global irradiance exceeded 200 W/m^2. The expression of the PV power could be given as:

$$E_{pv} = 0.127\cdot E_{vg} \quad (10)$$

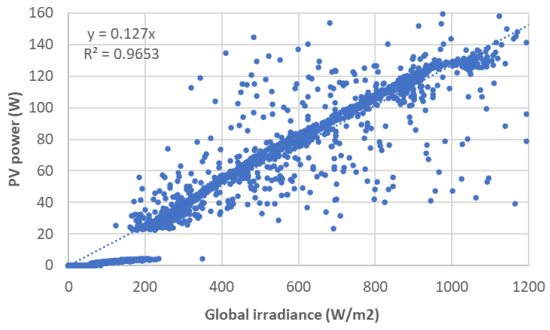

Figure 7. The PV power from the slats and the global solar irradiance.

3.2 Performance assessment

Daylighting performance of the PV slats was assessed in two aspects: the interior daylight illuminance and the energy saving potential. The experimental chamber with a south facing window was chosen to be the demonstration case.

a) Slat adjustment

The slat position strongly influenced not only the interior daylight illuminance but also the visual quality in the daylit space. For this system prototype, the slats could rotate counterclockwise from the horizontal position (0°) to the perpendicular position (90°) and could rotate clockwise from the horizontal position to its limit angle of 30°. According to the diagram in Fig. 8, the angle was assigned to be positive ($+\theta$) when the slat rotated counterclockwise from the horizontal, and to be negative ($-\theta$) when the slat rotated clockwise from the horizontal.

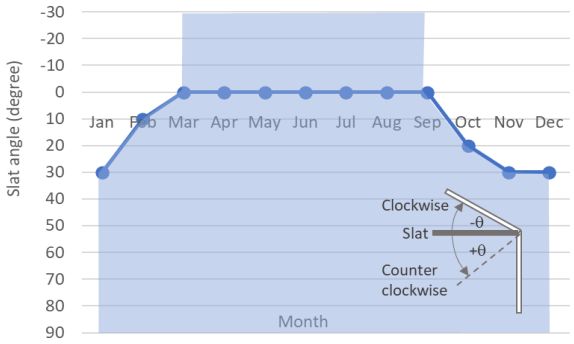

Fig. 8: The PV slat adjustment scheme.

To reap a full benefit of the daylighting, the PV slats were set to the shallowest angle that maximized the exterior view and perfectly intercepted the direct sunlight to prevent the potential occurrence of the visual discomfort glare. Based on the slat configuration (slat width and separation) and the sun path at the study site, the monthly slat setting according to the scheme mentioned above could be presented by the dotted line in Fig. 8. The slats were at 0° from May to September and were tilted to 30° from December to January when the sun appeared in front of the window with low elevation. The shaded area in the plot presents the possible tilted angle of the slats sufficient to completely intercept the beam solar irradiance on the windowpane.

b) Exterior daylight and solar irradiance

Availability of the exterior daylight and solar irradiance at a location is the primary data necessary for the performance assessment. In this study, the available daylight and solar irradiance were obtained from the records at our meteorological station.

As observed by the numerical data in Table 2, the global daylight illuminance was quite similar for all twelve months. The monthly mean hourly values of the global daylight were higher than 30 klux since 8:00 in morning and were peak at 90 klux at noon. The total daylight on the south façade influenced by the sun position of which the values were highest in December when the sun stays at low altitude. The total daylight on the south was lowest in June when the sun is due north so there was only diffuse component presented.

c) Transmitted and workplane daylight

Based on the daylight data in Table 2, the hourly mean values of the transmitted daylight from the window (E_{vT}) could be determined by using Eq. (8). The workplane daylight at the five points along the room depth (E_i) could then be determined by using Eq. (9). The calculated results for March, June, September, and December were selected to present in Table 3. According to the slat adjustment scheme in Fig. 8, the transmitted and the workplane daylight illuminance were lowest in June when the sun stayed due north, opposite to the window facing orientation. The

daylight illuminance in equinox March and September increased almost double from that of June. It should be noticed that the interior daylight was highest in solstice December when the sun travelled at low elevation in front of the window even though the slats were rotated with the largest tilted angle (30°) to completely shade the sunlight. Overall, the workplane daylight from the windowed wall deep to the middle of the room (50%D) were higher than 300 lux for most office hours.

The electrical energy use from lighting was considered for two scenarios: the typical office and the low-energy office.

Uniform lighting is the present lighting design norm for all typical office buildings where electric lamps were installed on ceiling to distribute the uniform illumination level of 500 lux on the workplane level (0.75 m above floor) for the whole working space. All lamps were fully on during the regular office hours from 8:00-17:00, regardless of the available exterior daylight.

d) Electricity use for lighting

Table 2. The available daylight illuminance (klux) and solar irradiance (W/m^2) during the office hour 8:00-17:00 of Bangkok

Month	Jan	Feb	Mar	Apr	May	Jun	Jul	Aug	Sep	Oct	Nov	Dec
Global daylight illuminance (klux)												
8:00	26.1	30.0	37.6	42.6	42.3	39.2	40.7	38.7	35.9	34.7	33.5	31.2
9:00	46.0	51.2	59.3	62.9	60.8	57.9	58.7	58.8	56.2	55.1	56.7	52.5
10:00	64.2	68.5	72.9	74.9	74.1	71.8	72.8	74.1	70.7	72.1	74.7	69.5
11:00	72.8	76.5	79.0	82.5	79.8	81.7	79.9	82.0	79.4	76.9	83.3	80.0
12:00	75.1	78.5	83.2	83.8	76.4	82.7	81.0	83.7	81.1	78.8	84.0	82.2
13:00	69.7	72.8	75.9	80.7	74.0	78.2	77.7	78.5	76.7	72.3	78.1	75.1
14:00	59.0	63.4	67.8	69.2	65.9	66.2	69.8	68.0	66.5	61.3	65.4	63.7
15:00	43.1	49.3	53.1	57.2	54.6	53.5	53.7	52.4	49.6	46.5	49.2	46.0
16:00	24.5	29.4	34.9	37.5	37.4	35.8	35.1	33.7	29.0	28.0	29.5	25.9
17:00	7.1	9.9	14.5	17.6	17.2	17.2	17.5	14.7	12.0	10.4	9.4	7.2
Total daylight illuminance on south façade (klux)												
8:00	14.3	12.4	12.7	10.2	9.0	8.8	8.6	9.3	12.7	20.5	28.3	27.6
9:00	29.9	26.1	22.4	15.7	12.1	12.1	12.5	14.3	20.2	30.1	43.4	44.4
10:00	44.8	36.0	29.2	19.7	14.5	14.7	15.4	17.9	26.5	37.9	53.1	55.2
11:00	51.5	42.7	32.4	22.8	15.9	16.3	17.5	21.2	29.8	39.7	57.2	62.5
12:00	54.9	44.0	34.5	23.7	15.9	17.2	18.0	23.2	31.2	40.4	56.7	63.6
13:00	52.6	43.4	33.9	23.3	15.9	17.2	17.9	23.3	30.2	37.7	52.9	60.5
14:00	47.6	39.9	30.8	20.8	14.5	15.8	16.9	20.4	27.1	33.1	46.1	54.0
15:00	39.4	34.9	27.2	17.3	12.9	13.6	14.4	16.4	21.6	26.5	37.7	43.2
16:00	27.5	25.6	20.2	12.6	10.3	10.5	10.8	12.0	13.8	17.3	26.2	28.7
17:00	11.7	12.6	11.6	7.6	6.4	6.4	7.1	7.0	6.5	6.8	8.8	9.9
Global solar irradiance (W/m^2)												
8:00	138.8	154.5	216.9	279.6	290.5	265.0	255.9	240.1	243.8	262.2	249.5	203.3
9:00	302.8	337.4	404.9	461.5	453.2	425.3	417.2	415.7	414.4	433.7	443.1	390.5
10:00	487.3	503.5	563.2	592.2	587.3	568.7	561.5	564.2	560.5	588.8	603.3	548.2
11:00	598.8	628.3	650.3	688.7	663.4	668.1	654.2	663.0	644.6	639.2	687.5	661.9
12:00	656.7	664.4	704.3	714.9	654.3	709.1	686.7	702.0	686.2	658.4	699.2	694.2
13:00	633.7	653.4	685.1	695.9	631.7	682.8	667.9	675.2	653.0	604.7	646.5	654.0
14:00	554.9	582.7	596.8	604.2	569.6	582.0	614.1	595.0	569.8	506.2	533.2	552.9
15:00	430.9	481.6	505.6	504.2	471.4	467.7	497.6	468.8	434.4	375.7	392.7	406.1
16:00	274.6	326.5	347.8	346.9	331.6	329.8	335.8	321.8	259.6	223.3	229.5	238.0
17:00	111.9	150.0	182.5	178.9	166.3	172.6	188.1	158.8	117.7	82.2	68.8	76.8

Table 3. Transmitted daylight and workplane daylight illuminance from the PV slat system.

Time	Transmitted daylight (klux)				Daylight at 10% depth (lux)				Daylight at 50% depth (lux)				Daylight at 90% depth (lux)			
	Mar	Jun	Sep	Dec	Mar	Jun	Sep	Dec	Mar	Jun	Sep	Dec	Mar	Jun	Sep	Dec
8:00	2.9	2.0	2.9	5.5	991.2	682.4	987.3	1,866.6	152.3	104.8	151.7	286.7	76.8	52.8	76.5	144.6
9:00	5.1	2.8	4.6	8.8	1,748.5	945.2	1,574.6	3,006.4	268.6	145.2	241.9	461.8	135.5	73.2	122.0	232.9
10:00	6.7	3.3	6.0	10.9	2,280.4	1,142.5	2,063.6	3,736.5	350.3	175.5	317.0	573.9	176.7	88.5	159.9	289.5
11:00	7.4	3.7	6.8	12.4	2,524.5	1,271.2	2,324.9	4,234.3	387.8	195.3	357.1	650.4	195.6	98.5	180.1	328.1
12:00	7.9	3.9	7.1	12.6	2,687.5	1,338.3	2,432.5	4,306.8	412.8	205.6	373.6	661.5	208.2	103.7	188.5	333.7
13:00	7.7	3.9	6.9	12.0	2,644.6	1,337.5	2,353.7	4,099.6	406.2	205.4	361.5	629.7	204.9	103.6	182.4	317.6
14:00	7.0	3.6	6.2	10.7	2,399.0	1,232.2	2,109.6	3,655.9	368.5	189.3	324.0	561.6	185.9	95.4	163.4	283.3
15:00	6.2	3.1	4.9	8.6	2,122.1	1,061.4	1,684.6	2,925.8	326.0	163.0	258.8	449.4	164.4	82.2	130.5	226.7
16:00	4.6	2.4	3.1	5.7	1,572.3	819.7	1,073.9	1,943.1	241.5	125.9	165.0	298.5	121.8	63.5	83.2	150.5
17:00	2.6	1.5	1.5	2.0	904.7	497.6	507.7	667.8	139.0	76.4	78.0	102.6	70.1	38.5	39.3	51.7

Table 4. Electricity consumption from the task-ambient lighting.

Time	Electricity use for ambient lighting													Electricity use for task lighting (kWh_{elec})	Total electricity use (kWh_{elec})
	Zone at 10% depth (Wh_{elec})				Zone at 50% depth (Wh_{elec})				Zone at 90% depth (Wh_{elec})				All zones (kWh_{elec})		
	Mar	Jun	Sep	Dec	Mar	Jun	Sep	Dec	Mar	Jun	Sep	Dec	Year	Year	Year
8:00	0.0	0.0	0.0	0.0	306.4	404.7	307.6	27.6	462.8	512.4	463.4	322.1	14.8	5.0	19.82
9:00	0.0	0.0	0.0	0.0	65.2	321.0	120.6	0.0	341.1	470.2	369.1	139.0	9.1	5.0	14.03
10:00	0.0	0.0	0.0	0.0	0.0	258.2	0.0	0.0	255.6	438.5	290.5	21.7	6.4	5.0	11.34
11:00	0.0	0.0	0.0	0.0	0.0	217.2	0.0	0.0	216.4	417.8	248.5	0.0	5.2	5.0	10.22
12:00	0.0	0.0	0.0	0.0	0.0	195.8	0.0	0.0	190.2	407.0	231.2	0.0	4.9	5.0	9.83
13:00	0.0	0.0	0.0	0.0	0.0	196.1	0.0	0.0	197.1	407.2	243.9	0.0	5.1	5.0	10.04
14:00	0.0	0.0	0.0	0.0	0.0	229.6	0.0	0.0	236.6	424.1	283.1	34.6	6.1	5.0	11.05
15:00	0.0	0.0	0.0	0.0	0.0	284.0	85.5	0.0	281.1	451.5	351.4	151.9	7.9	5.0	12.92
16:00	0.0	0.0	0.0	0.0	121.3	361.0	280.0	3.2	369.4	490.4	449.5	309.8	12.0	5.0	16.98
17:00	0.0	0.0	0.0	0.0	333.9	463.6	460.4	409.4	476.7	542.1	540.5	514.8	20.2	5.0	25.17

By applying Eq. (7) with the assumptions of 40 working hours per week and 52 weeks per year, the annual electricity use from the lighting could be simply calculated at 655 kWh_{elec}/year for the experimental room with the area of 27 m^2.

Low energy buildings are established as a decarbonization strategy in building sector. Various measures of renewable energy and energy efficiency are implemented to achieve a deep energy conservation (reducing energy consumption by at least 70% from the baseline). Task-ambient lighting is an energy-efficient concept widely adopted to conserve lighting energy by which the workplane illuminance of 500 lux is targeted only at the working stations. The ambient lighting at a lower level of 300 lux is provided for circulating area using mainly the daylight from the shaded window. Electric light from the dimmable LED lamp will supplement to the daylight when it was not sufficient to meet the requirement of 300 lux.

As example, Table 4 presents that the hourly values of the required electrical energy of the ambient lighting (300 lux) for the three selected zones of 10%D, 50%D, and 90%D with the four selected months (in unit of Wh_{elec}). The selected zones and months were identical to that of Table 3. It is obvious that the electric lighting was not required at the zone near the window (10%D) as the daylight was sufficient for the whole working period. However, the electric lighting would increase in the deeper zones and in early morning and late afternoon. Dependency of the electricity consumption on the slats control and the sun position is also observed from the data from the four calendar months. With the hourly electricity use data of all five zones (in Table 4), the annual consumption of the ambient lighting for the experimental room was equal to 91.6 kWh_{elec}/year.

To determine the electricity use of task lighting, the typical occupancy design value of 0.1 person/m2 and the assumed working space of 2 m2/person were adopted, so the total area of the working station in the experimental room was approximated by 6 m2. The additional electric lighting of 200 lux was provided for this area to meet the target illuminance of 500 lux, as another 300 lux was already obtained by the ambient lighting. As shown in Table 4, the annual electricity consumption of the task lighting was 49.8 kWhelec/year. Hence, the total energy from the task lighting and the ambient lighting was calculated at 141.41 kWhelec/year.

As this analysis also considered the indirect energy use from air-conditioning due to the heat dissipated from electric lamps, the total energy for lighting would be equal to 188.54 kWhelec/year. This indirect energy was relied on the air-conditioning performance where the COP of 3.0 was given.

e) PV power generation and energy surplus

In this study, the upper surfaces of the external slats were equipped with the flexible PV cells for the onsite power generation. Based on the empirical Eq. (10), the hourly electrical energy from the PV slats could be calculated, and the results were presented in Table 5.

The annual energy generated from the PV slats was 214.51 kWhelec/year, which was larger than the required energy for lighting (188.54 kWhelec/year). It should be remarked that the power generation was calculated from the whole days including weekend (Saturday and Sunday), that was distinct from the lighting energy calculation made based on five working days a week.

It can be observed from the hourly data in Tables 4 and 5 that the solar generation did not well match to the required electrical lighting energy, thus battery bank was essentially installed to store excessive electricity to serve during the deficit periods. The results in Table 5 show that the PV slats with battery storage could provide the required energy for lighting and supply the surplus electricity of 71.6 kWhelec/year to the experimental office room.

Table 5. Electricity generation from the PV slats and its energy surplus.

Time	Generated electricity from the PV slats (kWh_{elec})					Energy surplus (kWh_{elec})
	Mar	Jun	Sep	Dec	Year	
8:00	0.83	1.01	0.93	0.77	10.67	-9.2
9:00	1.54	1.62	1.58	1.49	18.67	4.6
10:00	2.15	2.17	2.14	2.09	25.64	14.3
11:00	2.48	2.55	2.46	2.52	29.90	19.7
12:00	2.68	2.70	2.61	2.64	31.36	21.5
13:00	2.61	2.60	2.49	2.49	30.04	20.0
14:00	2.27	2.22	2.17	2.11	26.14	15.1
15:00	1.93	1.78	1.65	1.55	20.71	7.8
16:00	1.32	1.26	0.99	0.91	13.58	-3.4
17:00	0.70	0.66	0.45	0.29	6.30	-18.9

4. Conclusion

The daylighting performance of the south-facing window with the external PV slats was investigated through the experiments. By conducting the measurements under varying conditions of the real sky, the empirical relationships could be formulated to determine the transmitted daylight from the window and the workplane daylight distribution with the slat angle for the daylit room. The solar power of the PV slats was also developed as a function of the global solar irradiance.

As the study site is situated in the tropical zone where the sun travels in all directions, this study introduced a simple scheme of the angle adjustment for the PV slats to fully intercept the sunlight whilst maximizing the exterior view for the daylighting. The task-ambient lighting concept was also deployed for enhancing energy conservation for the office lighting.

By using the experimental room as the demonstration case, the workplane daylight illuminance from the PV slats could be assessed for the whole year using the developed relationships and the local daylight and solar irradiance database. The required artificial light from electric lamps to supplement the workplane daylight illuminance was then determined. The analysis showed that the daylighting of the PV slat system could save the lighting energy by up to 80% compared to the typical office case designed based on the uniform lighting concept. The generated solar energy from the PV array of the shading slats was estimated to be sufficient for the lighting by the direct-current LED lamps. However, battery store was required due to the time mismatch between the solar power generation and the required electricity for supplement lighting.

List of Symbols

D	Room depth
S_i	Surface *i*
M_i	Exitance of surface *i*
M_{di}	Direct exitance of surface *i*
E_i	Illuminance of surface *i*
E_{di}	Direct illuminance of surface *i*
E_w	Work plane illuminance
E_{vT}	Transmitted daylight illuminance
F_{ij}	Form factor from surface *i* to *j*
C_i	Configuration factor of surface *i*
ρ_i	Reflectance of surface *i*
τ_w	Transmittance of window
LLF	Light loss factor

CU	Coefficient of utilization
LPD	Lighting power density
COP	Coefficient of performance
A_f	Floor area
E_{vg}	Global daylight illuminance
E_{vd}	Diffuse daylight illuminance
E_{vs}	Daylight illuminance on south facade
$E_{e,PV}$	Incident solar irradiance on PV cell
θ	Slat angle

References

[1] Abergel, T., Dean, B. Dulac, J. 2017. Towards a zero-emission, efficient, and resilient buildings and construction sector: Global Status Report 2017. UN Environment and International Energy Agency. Paris, France.

[2] Chirarattananon, S. and Chaiwiwatworakul, P. 2007. Distributions of sky luminance and radiance of North Bangkok under standard distributions, *Renewable Energy*, 32(8), 1328-1345, doi: 10.1016/j.renene.2006.06.004.

[3] Mettanant, V., Chaiwiwatworakul, P. and Chirarattananon, S. 2017. A model of Thai's sky luminance distribution based on reduced CIE standard sky types, *Renewable Energy*, 103, 739-749, doi: 10.1016/j.renene.2016.11.008.

[4] Chirarattananon, S., Chaiwiwatworakul, P. and Pattanasethanon, S. 2002. Daylight availability and models for global and diffuse horizontal illuminance and irradiance for Bangkok, *Renewable Energy*, 26, 69-89, https://doi.org/10.1016/S0960-1481(01)00099-4.

[5] Aste, N., Compostella, J. and Mazzon, M. 2012. Comparative energy and economic performance analysis of an electrochromic window and automated external venetian blind, *Energy Procedia*, 30, 404-413, doi: 10.1016/j.egypro.2012.11.048.

[6] Alzoubi, H.H. and Al-Zoubi, A.H. 2010. Assessment of building façade performance in terms of daylighting and the associated energy consumption in architectural spaces: Vertical and horizontal shading devices for southern exposure facades, *Energy Conversion Management*, 51(8), 1592-1599, doi: 10.1016/j.enconman.2009.08.039.

[7] Chaiwiwatworakul, P., Chirarattananon, S. and Rakkwamsuk, P. 2009. Application of automated blind for daylighting in tropical region, *Energy Conversion Management*, 50(12), 2927-2943, doi: 10.1016/j.enconman.2009.07.008.

[8] Fathoni, A.M., Chaiwiwatworakul, P. and Mettanant, V. 2016. Energy analysis of the daylighting from a double-pane glazed window with enclosed horizontal slats in the tropics, *Energy and Buildings*, 128, 413-430, doi: 10.1016/j.enbuild.2016.06.034.

[9] Ingabo, S.N., Chaiwiwatworakul, P. and Mettanant, V. 2020. Impact of adjustable external horizontal shading slats on indoor visual comfort in tropical climate, *Naresuan University Journal: Science and Technology (NUJST)*, 28(1), 23-37.

[10] Ingabo, S.N., Chirarattananon, S. and Chaiwiwatworakul, P. 2021. Application of external horizontal shading slats for daylighting through north-facing windows, *Science, Engineering and Health Studies*, 21040002, https://doi.org/10.14456/sehs.2021.7.

[11] Mandalaki, M., Zervas, K., Tsoutsos, T. and Vazakas, A. 2012. Assessment of fixed shading devices with integrated PV for efficient energy use, *Solar Energy*, 86(9), 2561-2575, doi: 10.1016/j.solener.2012.05.026.

[12] Taveres-Cachat, E., Lobaccaro, G., Goia, F. and Chaudhary, G. 2019. A methodology to improve the performance of PV integrated shading devices using multi-objective optimization, *Applied Energy*, 247, 731-744, doi: 10.1016/j.apenergy.2019.04.033.

[13] Sanati, L. and Utzinger, M. 2013. The effect of window shading design on occupant use of blinds and electric lighting, *Building and Environment*, 64, 67-76, doi: 10.1016/j.buildenv.2013.02.013.